Front. Med. 2024, 18(5): 862−877
https://doi.org/10.1007/s11684-024-1086-2

RESEARCH ARTICLE

Identification of susceptibility loci and relevant cell type for IgA nephropathy in Han Chinese by integrative genome-wide analysis

Ming Li[1,2,3,*], Xingjie Hao[4,*], Dianchun Shi[1,2,3,*], Shanshan Cheng[4], Zhong Zhong[2,5], Lu Cai[2,5], Minghui Jiang[4], Lin Ding[4], Lanbo Ding[4], Chaolong Wang (✉)[4,#], Xueqing Yu (✉)[1,2,3,#]

[1]Department of Nephrology, Guangdong Provincial People's Hospital (Guangdong Academy of Medical Sciences), Southern Medical University, Guangzhou 510080, China; [2]Department of Nephrology, The First Affiliated Hospital, Sun Yat-sen University, Guangzhou 510080, China; [3]Guangdong-Hong Kong Joint Laboratory on Immunological and Genetic Kidney Diseases, Guangzhou 510080, China; [4]Department of Epidemiology and Biostatistics, Ministry of Education Key Laboratory of Environment and Health, School of Public Health, Tongji Medical College, Huazhong University of Science and Technology, Wuhan 430030, China; [5]NHC Key Laboratory of Nephrology (Sun Yat-sen University), and Guangdong Provincial Key Laboratory of Nephrology, Guangzhou 510080, China

Abstract **Although many susceptibility loci for IgA nephropathy (IgAN) have been identified, they only account for 11.0% of the overall IgAN variance. We performed a large genome-wide meta-analysis of IgAN in Han Chinese with 3616 cases and 10 417 controls to identify additional genetic loci of IgAN. Considering that inflammatory bowel disease (IBD) and asthma might share an etiology of dysregulated mucosal immunity with IgAN, we performed cross-trait integrative analysis by leveraging functional annotations of relevant cell type and the pleiotropic information from IBD and asthma. Among 8 669 456 imputed variants, we identified a novel locus at 4p14 containing the long noncoding RNA *LOC101060498*. Cell type enrichment analysis based on annotations suggested that PMA-I-stimulated $CD4^+CD25^-IL17^+$ Th17 cell was the most relevant cell type for IgAN, which highlights the essential role of Th17 pathway in the pathogenesis of IgAN. Furthermore, we identified six more novel loci associated with IgAN, which included three loci showing pleiotropic effects with IBD or asthma (2q35/*PNKD*, 6q25.2/*SCAF8*, and 22q11.21/*UBE2L3*) and three loci specific to IgAN (14q32.32/*TRAF3*, 16q22.2/*TXNL4B*, and 21q21.3/*LINC00113*) in the pleiotropic analysis. Our findings support the involvement of mucosal immunity, especially T cell immune response and IL-17 signal pathway, in the development of IgAN and shed light on further investigation of IgAN.**

Keywords IgA nephropathy (IgAN); genome-wide association study (GWAS); relevant cell types; integrative analysis; pleiotropy

Introduction

IgA nephropathy (IgAN) is a common primary glomerulonephritis throughout the world. It is characterized by the deposition of IgA in the mesangial area of glomeruli and various histopathological lesions, including mesangial cell proliferation and accumulation of extracellular matrix [1]. IgAN shows a slow but persistent clinical course, and approximately 25%–50% of IgAN patients will develop into end-stage renal disease (ESRD) within 20 years after initial diagnosis [1]. The clinicopathologic patterns and the prognosis of IgAN show wide variability among patients. The gross hematuria often coincides with mucosal infections in either the upper respiratory tract or the gastrointestinal tract during the course of IgAN [2]. IgAN has led to substantial healthcare burden, and the prevalence of biopsy-proven IgAN shows a marked difference in various regions. Asian populations have the highest prevalence of 40%–50% of primary glomerulonephritis,

Received November 22, 2023; accepted May 17, 2024

Correspondence: Xueqing Yu, yuxueqing@gdph.org.cn;
Chaolong Wang, chaolong@hust.edu.cn

[*]Ming Li, Xingjie Hao, and Dianchun Shi contributed equally as the first author.

[#]Chaolong Wang and Xueqing Yu contributed equally as the corresponding authors.

which in contrast to 20%–30% in Europeans, 10%–20% in United States, and < 5% in Africans [1,3,4]. Although the precise pathogenesis of IgAN remains unclear, genetic and environmental factors are found to contribute to the susceptibility and disease progression of IgAN [5].

To date, seven genome-wide association studies (GWASs) for IgAN have been conducted, which have reported dozens of susceptibility loci for IgAN [5–11]. Interestingly, most of these loci are either associated with inflammatory bowel disease (IBD) or involved in the maintenance of the intestinal epithelial barrier [8,11,12]. Furthermore, loci associated with IgAN are significantly enriched in the KEGG pathways of intestinal immune network for IgA production and asthma, which suggests that IgAN, IBD, and asthma might share some common etiology [8]. Indeed, the recently proposed concept of mucosa–kidney axis highlights an essential role of dysregulated mucosal immunity in IgAN [13,14]. Moreover, most IgA antibodies, especially galactose deficient IgA1, were produced by the mucosal immune system, including the upper airway and the gut [15]. Notably, Nefecon, which is a novel enteric targeted-release formulation of budesonide (TRF-budesonide) directed to the mucosa-associated lymphoid tissue to modulate immune cell function and mucosa IgA production, has been applied as a specific treatment of IgAN. Consistent with the importance of intestinal mucosal immunity in the pathogenesis of IgAN, the NEFIGAN (NCT01738035) study has found that TRF-budesonide can reduce proteinuria and the risk of future progression to ESRD in IgAN patients [16]. However, the identified genetic loci together only explain about 11% of the disease risk of IgAN [11]. Increasing the sample sizes and genotyping density have been proven useful to identify novel susceptibility loci. Recent methodology advances in the integrative analysis; for instance, genetic analysis incorporating pleiotropy and annotation (GPA) [17] is powerful and cost effective in identifying the susceptibility loci by combining information from existing GWAS data of multiple related traits and functional annotations.

Previous GWASs of IgAN were mostly based on Chinese and had relatively moderate sample sizes [5–10], in contrast to other large-scale GWASs in Europeans, such as IBD and asthma [18,19]. In this study, we genotyped 1000 IgAN cases and 1000 healthy controls using the Illumina Infinium Omni2.5-8 BeadChip and obtained individual genotyping data from published IgAN GWASs in Han Chinese. We imputed all samples with a large Asian whole-genome sequencing reference panel [20] and performed a meta-analysis involving 3616 cases and 10 417 controls across 8 669 456 imputed variants after quality controls (QC). Based on the meta-analysis results, we performed enrichment analysis to identify the specific tissues and cell types relevant to the pathogenesis of IgAN. Finally, we applied the GPA method to discover additional IgAN susceptibility loci by leveraging pleiotropy shared with IBD and asthma, as well as genomic functional annotations from relevant cell types. By comprehensive GWAS and post-GWAS analyses, we aimed to advance the understanding of molecular mechanisms underlying the genetic predisposition of IgAN.

Materials and methods

Study subjects and genotyping data in previous studies

A large GWAS meta-analysis was performed for this study. We collected individual-level genotype data from two published IgAN GWASs of Han Chinese population [9,10]. For each dataset, we used PLINK [21] to perform a series of standard QC: excluding monomorphic single nucleotide polymorphisms (SNPs) and SNPs on sex chromosomes, with missing rate > 0.05 or *P* value for Hardy–Weinberg equilibrium (HWE) $< 10^{-6}$, and excluding samples with > 0.1 missing genotypes. Details for the two datasets are provided below.

(1) Dataset 1. We downloaded the dataset of Gharavi *et al*.'s study [10] from dbGaP (accession numbers: phs000431.v1.p1 and phs000431.v2.p1), which consisted of 1194 cases and 902 controls genotyped on the Illumina Human 610 Quad BeadChip. After lifting over to GRCh37, 486 809 autosomal SNPs were obtained. QC procedures removed one duplicated SNP and 346 SNPs failing in the HWE test, which resulted in 486 462 SNPs for further analyses.

(2) Dataset 2. The second dataset was from our previous study [9], including 1434 cases and 10 661 controls genotyped on various Illumina GWAS arrays. We excluded 2098 controls genotyped on the Illumina OmniExpress array, given that the number of overlapping sites across all arrays would be substantially reduced if the OmniExpress array data were included. The number of overlapping autosomal SNPs for the remaining samples was 407 694. We excluded additional nine samples due to missing rate > 0.1 and 564 SNPs failing in HWE tests, which resulted in 1434 cases and 8554 controls genotyped on 407 130 SNPs.

Genotyped study subjects in the current study

We newly genotyped 1000 IgAN cases and 1000 controls using Illumina Infinium Omni2.5-8 BeadChip, which covered 2 368 775 SNPs across the genome after removing duplicated sites (Dataset 3). All IgAN patients were histopathologically diagnosed by kidney biopsy, and patients with secondary IgAN, including Henoch–Schonlein purpura, systemic lupus erythematosus, HIV

infection, or other autoimmune diseases, were removed. Baseline demographic and clinical data for IgAN patients were collected at the time of diagnosis. After removing 15 samples due to > 0.1 missing rate, 10 249 SNPs due to > 0.05 missing rate, 3930 SNPs failing in the HWE test, 759 111 monomorphic SNPs, and 34 030 SNPs on sex chromosomes, the final dataset consisted of 995 cases and 990 controls genotyped on 1 561 455 SNPs.

This study was approved by the Institutional Review Board at the Guangdong Provincial People's Hospital and the First Affiliated Hospital of Sun Yat-sen University according to the Declaration of Helsinki. Informed consent form was obtained from all study subjects.

Source of IBD and asthma summary statistics

GWAS summary statistics of asthma for 7 488 535 variants were from the GWAS of 14 085 cases and 76 768 controls of European ancestry from the UK Biobank [19]. GWAS summary statistics of IBD for 11 555 663 variants were downloaded from the GWAS of 38 155 cases and 48 485 controls of European ancestry [18].

Principal component and family relatedness analysis

We extracted 192 162 shared SNPs across the three post-QC IgAN datasets and merged the datasets. We then used PLINK [21] to prune the SNPs by removing SNPs with linkage disequilibrium (LD) ($r^2 > 0.2$) within 1 Mb, which left 68 920 independent SNPs with MAF > 0.01 for relatedness check and principal component analysis (PCA). No cryptic relatedness was observed in the first two datasets because relatedness had been removed in the previous studies [8,10]. For the newly genotyped samples, we used PLINK to calculate pairwise identity-by-descent, and we randomly removed one individual from each pair with individuals with close relatedness ($\hat{\pi} \geqslant 0.177$). This step removed seven cases and 29 controls, which left 988 cases and 961 controls of Dataset 3. Finally, we performed PCA for the remaining unrelated 3616 cases and 10 417 controls from the three datasets [21]. The top 10 PCs were visually inspected and used to adjust for population structure in the association analyses.

Genotype imputation

We performed genotype imputation using an Asian whole-genome sequencing reference panel, which consisted of 4441 Singapore Chinese, Malay, and Indian samples from the SG10K project [20] and 998 East Asian and South Asian samples from the 1000 Genomes Project (1KGP) [22]. Our previous study suggested that the combined reference panel of SG10K and 1KGP could improve the accuracy of imputation [20]. We imputed each of the three genotyping datasets separately. After excluding SNPs that had different alleles from the imputation reference panel, we first phased each genotyping dataset with the imputation reference panel using EAGLE2 [23]. Then, we performed imputation using Minimac4 [24]. After removing variants with MAF < 0.005, P value of HWE < 10^{-6}, and imputation $R^2 < 0.3$ using bcftools (version 1.10.2) [25], 8 669 456 biallelic variants (including SNPs and INDELs) shared by three imputed datasets were retained for downstream analyses.

Association analysis

For each of the three imputed datasets, we performed single-variant association test between IgAN and the imputed dosage using the Wald test of logistic regression implemented in EPACTS. The top 10 PCs were included as covariates to adjust for the potential population structure. We then combined the results using fixed effect inverse-variance-weighted meta-analysis implemented in METAL [26]. The LD scores were estimated based on reference genotypes of East Asian (EAS) samples in the 1KGP [22]. SNPs in the major histocompatibility complex (MHC) region (i.e., chromosome 6, 25–35 Mb) were removed for LD score regression (LDSC). The meta-analysis summary statistics were adjusted for the intercept of LDSC to correct the potential uncorrected confounding induced by population stratification [27]. FUMA [28] was used to define the genomic risk loci by clumping and obtain functional information of the SNPs in these loci. We identified the independent significant SNPs that had a P value < 5×10^{-8} and were independent from each other at $r^2 < 0.1$. Except for the MHC region, the genomic risk loci were defined by identifying physical regions in LD with these independent significant SNPs in 1 Mb region.

Identification of cell types relevant to specific traits

We first performed MAGMA gene-property analysis on the FUMA platform [28] to identify tissue specificity of IgAN for identifying relevant cell types, which was based on the gene expression data from the GTEx project [29]. The variant-level P values were transformed into gene-level Z scores using MAGMA. The association of gene-level Z scores with gene expression in each tissue or cell type was tested to identify relevant tissues or cell types. A Bonferroni correction was applied to account for multiple testing. Then, the stratified LDSC was applied to evaluate if the heritability of a trait was enriched in genomic functional regions specific to particular cell types. We downloaded tracks of GenoSkyline-Plus annotations specific to particular cell types [30], including 66 tracks used in the original GenoSkyline study [30] and one additional track for the kidney. A binary annotation was

created for each cell type, which indicated whether an SNP resided in the tracks of GenoSkyline-Plus annotations specific to particular cell types. We excluded the MHC region and included 53 baseline annotations as suggested in the stratified LDSC model [31]. The coefficient *P* value was selected as a measure of the association of the cell type with the trait. Specifically, the LD scores were calculated based on the genotypes of EAS sample from 1KGP [22] for IgAN and European (EUR) samples from 1KGP [22] for IBD and asthma. After identifying cell types relevant to IgAN by LDSC, we further explored the distribution of IgAN signals in different chromatin states [32] of the relevant cell types. The enrichment was defined as the ratio of the proportion of significant variants in a certain chromatin state track and the proportion of all variants in the corresponding chromatin state track. The Fisher's exact test for a 2 × 2 table was used for the enrichment test.

GPA analysis

We extracted 5 033 499 autosomal SNPs shared by the GWAS summary statistics of IBD [18], asthma [19], and IgAN. We first selected the independent ($r^2 < 0.1$) lead SNP in each locus showing suggestive association with any of the three traits ($P < 10^{-5}$). Then, we selected the approximately LD independent SNPs by thinning SNPs to at least 2 kb apart based on the genotypes of EAS sample from 1KGP [22], and 945 405 SNPs were left for GPA analysis. We incorporated GenoSkyline-Plus annotation tracks of PMA-I-stimulated $CD4^+CD25^-IL17^+$ Th17 cells as the relevant cell type for IgAN, IBD, and asthma in the GPA integrative analysis. The arguments of association pattern could be set as "1" and "*," which indicate the phenotype of interest and non-interest. For pair-wise analyses between IgAN and IBD and between IgAN and asthma, the pleiotropic test for each variant was conducted by setting the pattern as "11." However, the association test for IgAN was conducted by setting the pattern as "1*." Thus, the loci identified by the association test included the pleiotropic loci for two traits and unique risk loci for IgAN. Notably, IBD and asthma GWAS summary statistics were based on European ancestry, while IgAN was from Han Chinese population. Thus, heterogeneity of genetic effect might exist. In addition, the summary statistics have been pruned to be approximately independent to represent the signals. Therefore, we sought to identify the risk regions instead of risk variants in the GPA integrative analysis. We identified the independent loci with variants passing the threshold of false discovery rate (FDR) 0.05 and independent from each other at $r^2 < 0.1$. The LD information was calculated using reference genotypes of EAS samples in 1KGP [22].

Colocalization analyses

For the novel loci identified by GPA, we further performed colocalization analysis using coloc [33] to detect whether a pair of diseases share a causal variant based on a window of 100 kb of the lead variants. A total of five hypotheses were assumed, including the H4 that a causal variant was shared. A pair of diseases were considered to be colocalized if the posterior probability of H4 (PP4) was larger than 0.7. The colocalization results were plotted using the Locus Compare R package [34].

Analysis of clinical phenotypes and prognosis of IgAN

The top variants at the seven novel loci were selected to study their associations with the clinical phenotypes. The continuous variables were shown as median (interquartile range), and the category variables were expressed as number (percentage). For the genotype–phenotype association analysis, we used the logistic regression for binary and ordinal variables and linear regression for continuous variables. The Cox proportional hazard model was performed for the survival analysis. In addition, we calculated the polygenic risk score (PRS) of IgAN using the significant and independent variants at the loci identified by GWAS meta-analysis and GPA integrative analysis. The SNP information used in PRS is shown in Table S1. Then, we tested the associations between the clinical phenotypes and PRS of IgAN. All analysis was performed using R version 4.1.3.

eQTL and functional annotation analysis

The eQTL analysis was based on the GTEx website. The Functional Mapping and Annotation (FUMA [28]) and Ensembl were also used to annotate the variants at the susceptibility loci. In addition, PolyPhen-2 and SIFT were used to investigate the potential effect of missense mutation on protein function. We also checked the functional annotation according to the CADD, RegulomeDB, and chromatin looping database.

Results

GWAS meta-analysis of IgAN in Han Chinese

We obtained Chinese GWAS data of IgAN from three sources: (1) published study by Gharavi *et al*. [10]; (2) our previous study by Li *et al*. [8]; and (3) newly genotyped samples in the present study. After QC (see details in "Materials and methods" section , Fig. S1), the sample sizes were 1194 cases and 902 controls in Dataset 1, 1434 cases and 8554 controls in Dataset 2, and 988 cases and 961 controls in Dataset 3, with a total of 3616 cases and 10 417 controls in the meta-analysis. PCA

found no obvious population stratification between cases and controls (Fig. S2). GWAS analysis with the top 10 principal components was applied to each dataset separately (Fig. S3), followed by inverse variance weighted meta-analysis for the 8 669 456 shared variants (Fig. 1) [26]. The intercept of LDSC was 1.031 (standard error (SE) = 0.008, Fig. S4), which indicates that the population structure was well controlled and the inflation was mostly due to polygenicity [27].

We identified six independent loci for IgAN ($P_{meta} < 5 \times 10^{-8}$, LD $r^2 < 0.1$), including five reported loci: *HLA* gene cluster at the MHC region, *DEFA* at 8p23.1, *ITGAX-ITGAM* at 16p11.2, *TNFSF13* at 17p13.1, and *HORMAD2* at 22q12.2 (Fig. 1, Table 1). Among non-MHC loci, we identified two novel missense variants at previously reported loci, which are rs2230429 (Pro517Arg, $P_{meta} = 1.33 \times 10^{-8}$) at *ITGAX* and rs11552708 (Gly67Arg, $P_{meta} = 7.66 \times 10^{-7}$) at *TNFSF13* (Table S2). We also examined the r^2 with two previously reported variants (rs1150612 and rs3803800) using the HaploReg v4.2 database, which showed that the rs2230429 was in strong LD with the rs1150612 ($r^2 = 0.93$) while the rs11552708 had no LD with the rs3803800. In particular, rs2230429 was predicted to be deleterious by PolyPhen2 [35] and SIFT [36] (Table S2). Furthermore, we identified one novel locus at 4p14 with the lead SNP rs11736377 ($P_{meta} = 4.17 \times 10^{-8}$) located 17 kb upstream of a long noncoding RNA (lncRNA) *LOC101060498* (Fig. S5). In our study, we also checked the previously reported loci of published IgAN GWASs [5–11]. We found that 58 of 60 variants were detected in our data and showed consistent effect direction, of which 52 had $P < 0.05$ (Table S3). These results suggest that our GWAS is consistent with those in previous studies.

Identification of relevant tissues and cell types for IgAN

Based on the GWAS summary statistics, we conducted MAGMA gene-property analysis to identify relevant tissues for IgAN [28]. Compared with gene expression profiles specific to 54 different tissues from the GTEx project [37], IgAN GWAS signals showed significant enrichment ($P = 5.46 \times 10^{-6}$) in genes expressed in the whole blood, rather than the kidney-related tissues (e.g., kidney cortex and kidney medulla, $P > 0.05$) (Fig. 2A). Next, we conducted stratified LDSC to pinpoint specific cell types relevant to IgAN, IBD, and asthma. Among GenoSkyline-Plus annotation tracks specific to 67 different cell types [30], PMA-I-stimulated $CD4^+CD25^-IL17^+$ Th17 cells were the only significant cell type for IgAN after multiple test correction ($P = 7.05 \times 10^{-5}$) and ranked the third for IBD ($P = 3.26 \times 10^{-4}$) and asthma ($P = 8.09 \times 10^{-5}$) (Fig. 2B). While most of the IgAN-associated variants were intergenic or intronic, they were significantly enriched in regions with regulatory function, including the flanking active transcription start site (TssAFlnk), enhancers (Enh), active transcription start site (TssA), and weak repressed PolyComb (ReprPCWk), among 14 chromatin states in PMA-I-stimulated $CD4^+CD25^-IL17^+$ Th17 cells ($P < 0.05/14$; Fig. S6). Furthermore, among 28 baseline annotations in the stratified LDSC, the heritability of IgAN was significantly enriched in super enhancer and H3K27ac-annotated regions ($P < 0.05/28$; Fig. S7).

Integrative analysis of IgAN, IBD, and asthma

The GPA method can boost the statistical power to identify IgAN signals by integrating pleiotropic information from GWAS of relevant traits and functional annotation from relevant cell types [17]. We performed GPA analyses for IgAN and IBD, as well as IgAN and asthma, both with functional annotation from the PMA-I-stimulated $CD4^+CD25^-IL17^+$ Th17 cells. In the joint analysis with IBD, we identified eight pleiotropic loci associated with IgAN and IBD, including two novel loci, namely, *PNKD* at 2q35 (rs1473901, false discovery rate $FDR_{11} = 0.013$, where the subscript 11 denotes pleiotropic association with both diseases) and *UBE2L3*

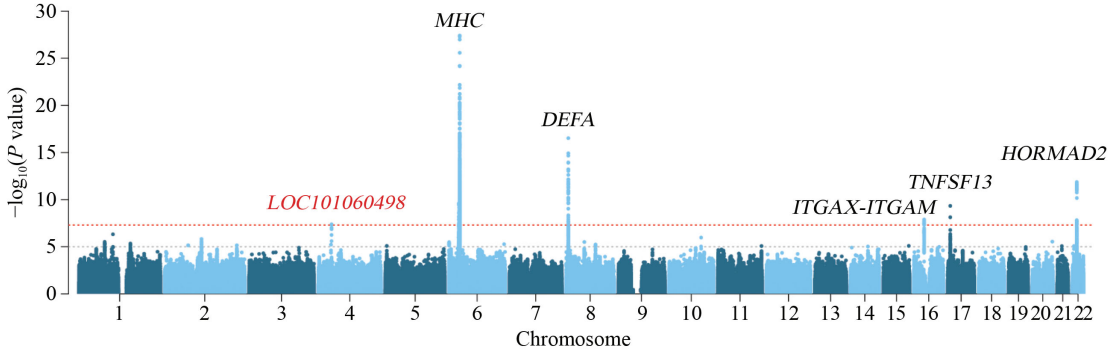

Fig. 1 Manhattan plot of the IgAN GWAS meta-analysis in Han Chinese. *P* values were adjusted for the intercept of LDSC. The red dash line indicates $P = 5 \times 10^{-8}$, and the gray dash line indicates $P = 10^{-5}$. Known IgAN loci are labeled in black, while novel loci are labeled in red.

Table 1 Significant loci associated with IgAN by GWAS meta-analysis

Locus	Lead variant[a]	Dataset	AF[b]	OR (95% CI)[c]	*P* value
4p14	rs11736377	Dataset 1	0.617	0.88 (0.76, 1.00)	5.49×10^{-2}
LOC101060498	chr4:40301264	Dataset 2	0.593	0.77 (0.71, 0.84)	4.58×10^{-9}
	T/C	Dataset 3	0.601	0.94 (0.83, 1.07)	3.64×10^{-1}
	Intergenic	Meta		0.83 (0.78, 0.89)	4.17×10^{-8}
MHC	rs9270599	Dataset 1	0.554	1.41 (1.24, 1.60)	1.78×10^{-7}
	chr6:32561656	Dataset 2	0.572	1.78 (1.56, 2.02)	1.42×10^{-18}
	A/G	Dataset 3	0.631	1.47 (1.29, 1.69)	2.47×10^{-8}
	Upstream	Meta		1.55 (1.43, 1.67)	3.94×10^{-28}
8p23.1	rs11137085	Dataset 1	0.543	1.35 (1.18, 1.54)	1.17×10^{-5}
DEFA	chr8:6877468	Dataset 2	0.504	1.30 (1.19, 1.41)	6.14×10^{-9}
	C/G	Dataset 3	0.505	1.39 (1.22, 1.59)	1.13×10^{-6}
	Upstream	Meta		1.33 (1.25, 1.42)	3.00×10^{-17}
16p11.2	rs13332545	Dataset 1	0.226	0.83 (0.72, 0.96)	1.44×10^{-2}
ITGAX-ITGAM	chr16:31377390	Dataset 2	0.293	0.80 (0.72, 0.89)	6.26×10^{-5}
	C/T	Dataset 3	0.317	0.78 (0.68, 0.89)	3.45×10^{-4}
	Intron	Meta		0.80 (0.75, 0.86)	1.29×10^{-8}
17p13.1	rs11078696	Dataset 1	0.680	0.84 (0.72, 0.97)	1.93×10^{-2}
TNFSF13	chr17:7459299	Dataset 2	0.641	0.82 (0.74, 0.90)	2.17×10^{-5}
	T/G	Dataset 3	0.632	0.72 (0.63, 0.83)	6.78×10^{-6}
	Intron	Meta		0.80 (0.75, 0.86)	4.63×10^{-10}
22q12.2	rs12537	Dataset 1	0.230	0.73 (0.63, 0.85)	3.09×10^{-5}
HORMAD2	chr22:30423460	Dataset 2	0.177	0.72 (0.64, 0.81)	5.94×10^{-8}
	T/C	Dataset 3	0.168	0.79 (0.66, 0.94)	6.51×10^{-3}
	3'UTR	Meta		0.74 (0.68, 0.80)	1.37×10^{-12}

[a]Variant with the smallest *P* value within each locus: rs number, GRCh37 genomic position, effect/non-effect alleles, and annotation of the variant. [b]AF: frequency of the effect allele. [c]Odds ratio (OR) and 95% confidence interval (CI) of the effect allele. Meta-analysis was based on inverse-variance weighted fixed-effect model. The *P* values of meta-analysis were adjusted by the intercept of LD score regression.

at 22q11.21 (rs1811069, FDR_{11} = 0.043) (Fig. 3A). Notably, six IgAN GWAS loci, including the newly reported loci *ZMIZ1* in the recent IgAN GWAS [11], showed significant pleiotropic effects with IBD. Furthermore, two more loci showed significant association specific to IgAN, including *TXNL4B* at 16q22.2 (rs77303550, FDR_{1*} = 0.045, where the subscript 1* denotes association with IgAN) and *LINC00113* at 21q21.3 (rs1811069, FDR_{1*} = 0.032) (Fig. 3B).

In the joint analysis with asthma, we identified three pleiotropic loci associated with IgAN and asthma (Fig. 3C), including one novel loci as *SCAF8* at 6q25.2 (rs10872710, FDR_{11} = 0.036). In addition, we identified one novel locus specific to IgAN: *TRAF3* at 14q32.32 (rs8004192, FDR_{1*} = 0.028) (Fig. 3D).

In summary, we identified six novel loci for IgAN by integrative analysis with GWAS summary statistics of IBD and asthma (Table 2). The original GWAS results at the six loci are presented in Fig. 4. The three pleiotropic loci showed similar association peaks in both diseases (Fig. 4A–4C), and they were colocalized with PP4 > 0.7 (Fig. S8A–S8C). Specifically, *PNKD* at 2q35 and *UBE2L3* at 22q11.21 were significant GWAS loci for IBD (Fig. 4A and 4B). Although *SCAF8* at 6q25.2 did not reach genome-wide significance in the original asthma GWAS, it displayed a noticeable regional peak (Fig. 4C). Finally, we observed regional peaks for IgAN, but these peaks were less obvious for IBD or asthma at the three novel loci specific to IgAN in the GPA analyses (Fig. 4D–4F). Moreover, no colocalized signal was observed (Fig. S8D–S8F).

Association with clinical characteristics and prognosis of IgAN patients

We collected the clinical and pathological characteristics of 2418 IgAN patients in Datasets 2 and 3 (Table S4). Then, we investigated the associations of clinical phenotypes with the lead variants of the seven novel loci and the PRS. We observed that the protective allele C of

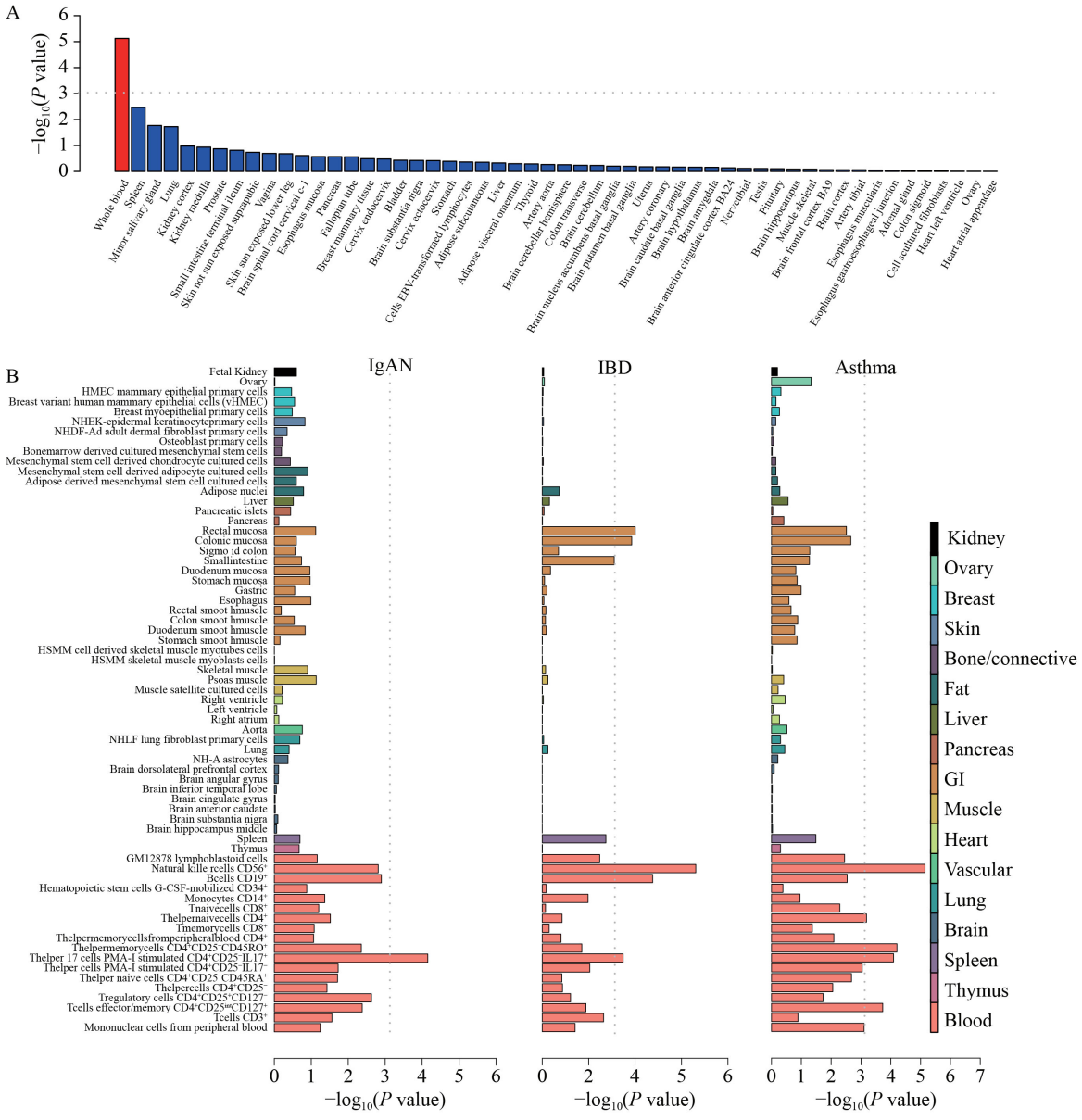

Fig. 2 Identification of tissues and cell types relevant to specific traits. (A) Relevant tissues of IgAN identified by MAGMA. The *x*-axis indicates 54 tissues from the GTEx Project, and the *y*-axis represents $-\log_{10}(P$ values) of enrichment test based on tissue-specific gene expression profiles. (B) Relevant cell types of IgAN, IBD, and asthma identified by the stratified LDSC. The *x*-axis indicates $-\log_{10}(P$ values) of the heritability enrichment test, and the *y*-axis indicates 67 cell types from the GenoSkyline-Plus annotation tracks. Dashed lines indicate the Bonferroni-corrected significance cutoffs (A, 0.05/54 = 0.00093; B, 0.05/67 = 0.00075).

rs1473901 at *PNKD* was associated with lower level of serum IgA (P = 0.017), and the protective allele T of rs77303550 at *TXNL4B* was correlated with milder proteinuria (P = 0.043) (Table S5). In addition, the PRS was found to be closely related with the increased proteinuria (P = 0.012), lower eGFR (P = 0.031), decreased C3 levels (P = 0.029), severe mesangial hypercellularity ($P = 5.2 \times 10^{-5}$), and segmental glomerulosclerosis (P = 0.039), respectively (Table S6). Follow-up data were available for 582 IgAN patients with a median follow-up time of 25.6 months, among whom 73 reached the endpoint of ESRD or doubled the serum creatinine after diagnosis. We applied Cox regression with adjustment for age, gender, hypertension, proteinuria, and eGFR (Tables S7 and S8). We found the correlation of the PRS with prognosis of IgAN (P = 0.011). No SNPs were associated with the prognosis of IgAN.

Functional investigation of the novel loci and variants

The seven novel loci identified by the present study

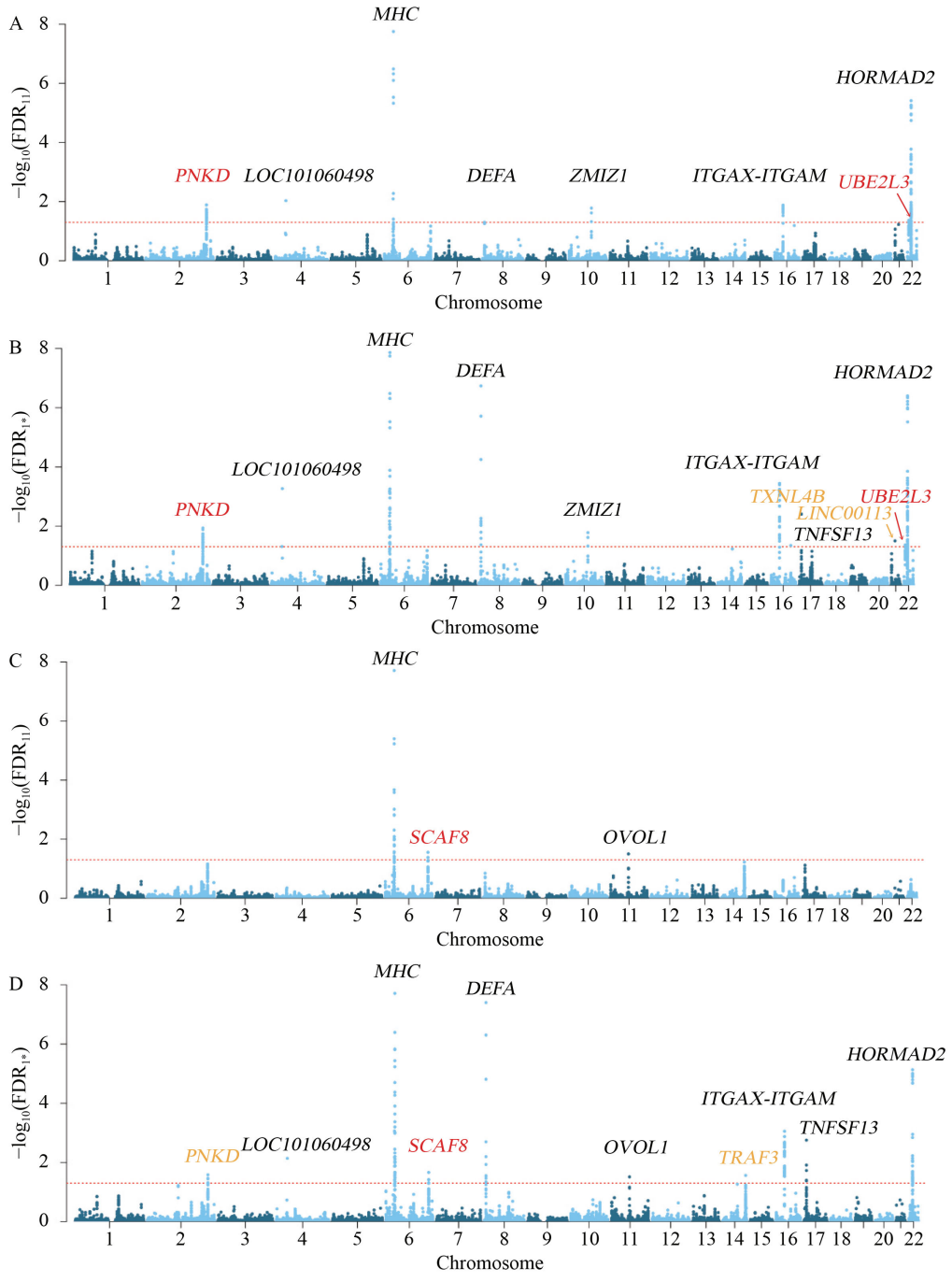

Fig. 3 IgAN risk loci identified by GPA analysis. (A) Manhattan plot of the pleiotropy test between IgAN and IBD. (B) Manhattan plot of the IgAN association test in the joint analysis of IgAN and IBD. (C) Manhattan plot of the pleiotropy test between IgAN and asthma. (D) Manhattan plot of the IgAN association test by the joint analysis of IgAN and asthma. The red dash line indicates the genome-wide significance level at FDR = 0.05. Gene names were labeled in black if they were significant in our IgAN meta-analysis or previous studies, in red if they were novel loci identified by the pleiotropic test, and in orange if they were novel IgAN specific loci. FDR_{11}, false discovery rate of the pleiotropy test; FDR_{1*}, false discovery rate of the association test.

included five protein coding genes and two long noncoding RNA genes, of which three lead variants were intergenic and four were intronic (Table 3). The lead variants at four novel loci are expression quantitative trait loci reported by the GTEx Project (Table S9). We also checked the functional annotation by using the CADD, RegulomeDB, and chromatin looping database (Table S10). Moreover, the variants that are highly correlated ($r^2 > 0.7$) with the seven lead SNPs and nominally significant ($P < 0.05$) at each novel locus were annotated

Table 2 Novel loci identified by GPA integrative analysis for IgAN

Loci	Type	FDR[a]	Lead SNP	P_{IgAN}	P_{IBD}	P_{Asthma}	Genes
2q35	IgAN and IBD	0.013	rs1473901	2.05×10^{-5}	5.35×10^{-8}	0.017	*PNKD*
22q11.21	IgAN and IBD	0.043	rs1811069	1.68×10^{-4}	6.21×10^{-10}	0.331	*UBE2L3*
6q25.2	IgAN and asthma	0.036	rs10872710	3.32×10^{-5}	0.655	1.33×10^{-4}	*SCAF8*
16q22.2	IgAN	0.045	rs77303550	2.10×10^{-5}	0.004	0.023	*TXNL4B*
21q21.3	IgAN	0.032	rs80271593	8.60×10^{-6}	0.007	0.418	*LINC00113*
14q32.32	IgAN	0.028	rs8004192	3.20×10^{-5}	0.663	0.002	*TRAF3*

[a]FDR, false discovery rate of pleiotropic test (FDR_{11}) for two traits or association test (FDR_{1*}) for IgAN. The GWAS *P* value of the lead SNP and the gene covering or close to the lead SNP at each locus are shown.

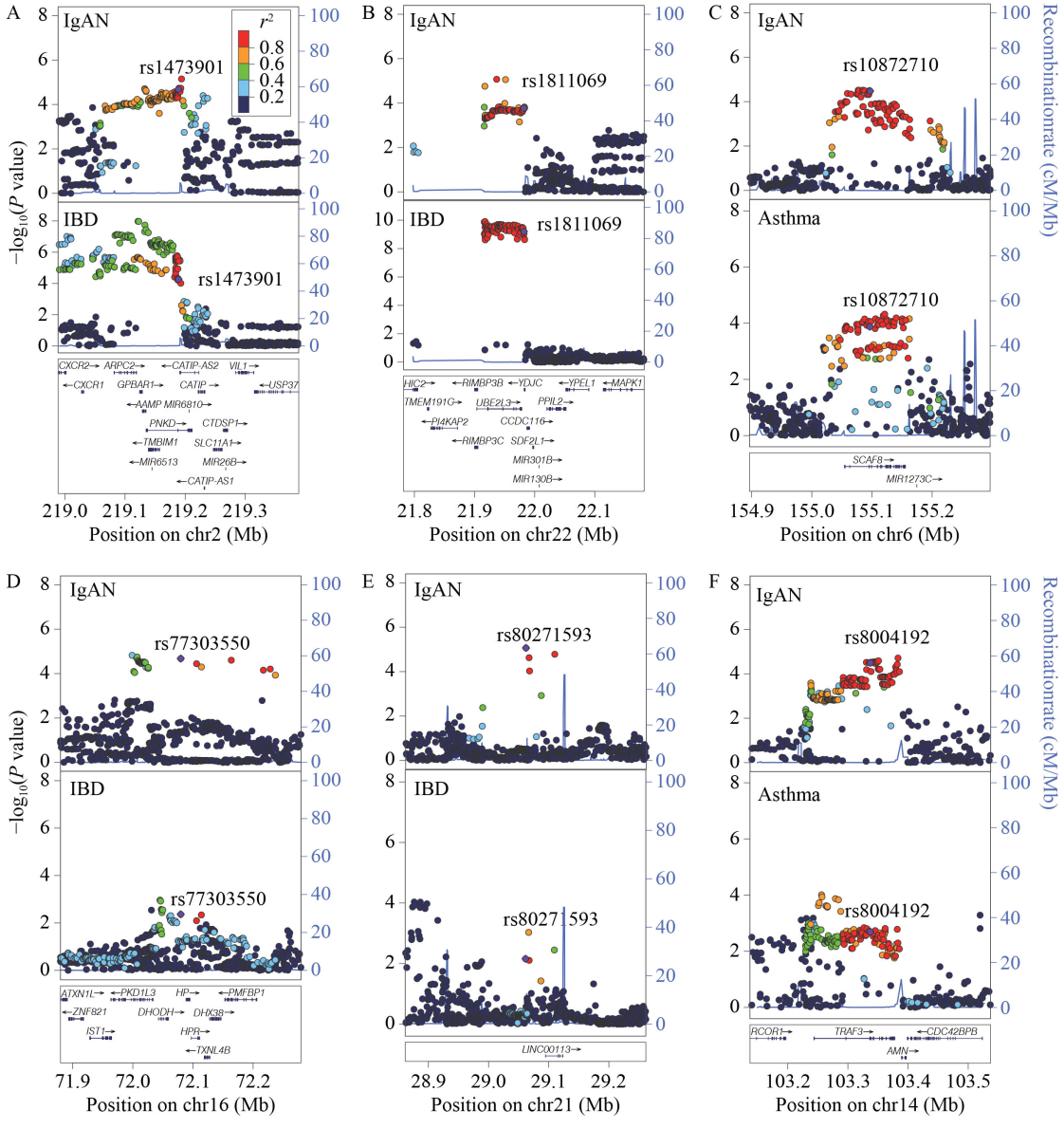

Fig. 4 Region plots of the original GWAS association *P* values for the six novel risk loci identified by GPA analysis. (A) Pleiotropic locus at 2q35 for IgAN and IBD. (B) Pleiotropic locus at 22q11.21 for IgAN and IBD. (C) Pleiotropic locus at 6q25.2 for IgAN and asthma. (D) IgAN specific locus at 16q22.2 by joint analysis of IgAN and IBD. (E) IgAN specific locus at 21q21.3 by joint analysis of IgAN and IBD. (F) IgAN specific loci at 14q32.32 by joint analysis of IgAN and asthma. At each locus, the lead variant in GPA analysis is indicated by the purple diamond, while neighboring variants are colored by their LD with the lead variant based on East Asians in the 1000 Genomes Project (color bar shown in panel A).

Table 3 Functional annotations of novel loci and associated SNPs

SNP/Locus	eQTL[a]	Associated diseases[b]	Gene function
rs11736377, 4p14, intergenic variant close to *LOC101060498*	No evidence for effects on gene expression levels	Vitiligo, Graves' disease, psoriasis, and autoimmune traits	*LOC101060498* is chromatin interacted with the adjacent immune-related gene *RHOH*, which is important for the development, migration, and signaling of T cells [40]. The involvement of *RHOH* in autoimmune-related diseases might be due to its ability to regulate T helper cell-induced cytokine production, especially in the Th17-cell differentiation [40]
rs1473901, 2q35, intron variant of *PNKD*	Associated with expression level of *PNKD* in blood, thyroid, skin, spleen, and liver	Inflammatory bowel disease, hematological traits (i.e., granulocyte count)	*PNKD* plays a role in regulation of myofibrillogenesis. The dysfunctional *PNKD* can reduce glutathione levels in cells and result in increasing oxidative stress levels, which has been linked to inflammation [69]
rs10872710, 6q25.2, intron variant of *SCAF8*	No evidence for effects on gene expression levels	Estimated glomerular filtration rate and diabetic nephropathy	*SCAF8* is the anti-terminator protein required to prevent early mRNA termination during transcription. *SCAF8* can suppress the use of early, alternative poly(A) sites, which prevents the accumulation of nonfunctional truncated proteins. *SCAF8* also acts as a positive regulator of transcript elongation [70]
rs1811069, 22q11.21, intergenic variant close to *UBE2L3*	Associated with expression level of *UBE2L3* in blood, mucosa, and muscularis of esophagus and skin	Inflammatory bowel disease, hepatitis B, systemic lupus erythematosus, and rheumatoid arthritis	*UBE2L3* encodes a member of the E2 ubiquitin-conjugating enzyme family involved in ubiquitin/proteasome-dependent degradation. The ubiquitin/proteasome pathway is involved in the development of multiple kidney diseases [53]
rs8004192, 14q32.32, intron variant of *TRAF3*	Associated with expression level of *TRAF3* in mucosa of esophagus, brain, and thyroid	Hematological traits, serum IgA level, systemic lupus erythematosus, multiple sclerosis, eczema, and asthma	*TRAF3* encoding a member of the TNF receptor associated factor protein family participates in the signal transduction of CD40 and plays a role in T cell dependent immune responses and the regulation of antiviral responses [61]. TRAF3 is required for normal signaling by the T cell antigen receptor, and cytoplasmic TRAF3 restrains nuclear factor κB activation in T and B cells [71]
rs77303550, 16q22.2, intron variant of *TXNL4B*	Associated with expression level of *TXNL4B* in cultured fibroblasts	Cardiovascular disease and type II diabetes mellitus	*TXNL4B* plays an essential role in pre-mRNA splicing and is required in cell cycle progression for S/G(2) transition [72]
rs80271593, 21q21.3, intergenic variant close to *LINC00113*	No evidence for effects on gene expression levels	Chronic renal failure	*LINC00113* promotes proliferation, survival, and migration by activating PI3K/Akt/mTOR signaling pathway in atherosclerosis [73]. It is downregulated in clear cell renal cell carcinoma samples compared with normal samples [74]

[a]eQTL is based on the database of GTEx. [b]The "Associated diseases" are based on known functional roles of the nearest gene.

based on the FUMA platform (Table S11). For example, rs1811069 at 22q11 is associated with the expression of *UBE2L3* in the whole blood, mucosa, and skin, while rs8004192 at 14q32 is associated with the expression of *TRAF3* in the mucosa of esophagus, brain, and thyroid. Notably, *UBE2L3* has been reported to associate with several immune diseases and involve in immune response pathways of which alterations can trigger autoimmune diseases. *TRAF3* plays an important role in T cell development and T cell dependent immune responses (Table 3).

Discussion

We have conducted a large genome-wide meta-analysis of IgAN in Han Chinese, involving 3616 cases and 10 417 controls. Followed by integrative analysis with GWAS summary statistics of IBD and asthma, we have discovered seven novel loci associated with IgAN, including one at 4p14 identified by meta-analysis and six by the GPA integrative analyses. Moreover, we have pinpointed the PMA-I-stimulated $CD4^+CD25^-IL17^+$ Th17 cells as the relevant cell type for IgAN. Our results imply that mucosal immunity and inflammation, especially T cell immune response and IL-17 signal pathway, play important roles in the pathogenesis of IgAN.

In the GWAS meta-analysis, we identified a novel locus at 4p14 with the lead SNP rs11736377 residing at 17 kb upstream of the lncRNA gene *LOC101060498*. Epigenomic annotations show that rs11736377 is in the active enhancer region of PMA-I-stimulated $CD4^+CD25^-IL17^+$ Th17 cells [32], which suggests that rs11736377 may regulate the expression of genes nearby. While the function of *LOC101060498* has not been fully studied in different tissues and cell types, recent three-dimensional genomic studies suggest that immune-related genes can interact with lncRNAs and form immune gene-priming lncRNAs for robust transcription [38]. Specifically, the Hi-C data of CD4 T cells [39] show that *LOC101060498* is chromatin interacted with the adjacent immune-related gene *RHOH*, which is involved in the T cell receptor-mediated signal transduction and plays an important role in T cell development and activation [40].

In addition, the lack of RhoH can stimulate T cell differentiation into Th17 cells in psoriasis-like chronic dermatitis [41]. RhoH has also been implicated in several other autoimmune diseases, such as psoriasis and systemic lupus erythematosus, by regulating T helper cell-induced cytokine production [40].

Remarkably, we found that GWAS signals of IgAN were significantly enriched in the functional regions of whole blood and PMA-I-stimulated $CD4^+CD25^-IL17^+$ Th17 cells. Interestingly, a recent GWAS study of IgAN also identified that PMA-I-stimulated primary T helper cells were one of the top enriched cell types in IgAN, which is consistent with our results [11]. While recent studies have highlighted the role of B cells and complement activation in IgAN, the essential role of T cells in the pathogenesis of IgAN has gained increasing attentions [42]. Th17 cells, which are characterized by the production of several cytokines (IL-17A, IL-17F, IL-22, and GM-CSF) and high CCR6 expression, played an important role in the early response to bacterial pathogens and in autoimmune diseases, such as nephritis and asthma [42,43]. As previously reported, the proportion of Th17 cell and the serum level of IL-17A were significantly higher in IgAN patients, and they were also associated with 24h proteinuria [44–46]. Furthermore, expression of IL-17A was found in renal tubule of IgAN patients with decreased renal function, severe proteinuria, and serious tubulointerstitial injury [47]. In addition, IL-17 could downregulate the mRNA expression of C1GALT1 and C1GALT1C1, which led to increased production of galactose deficient IgA1 [48]. Overall, Th17 cells and the serum level of IL-17 may be the aggravating factors in IgAN.

In addition to IgAN, cell type enrichment analysis also suggested that PMA-I-stimulated $CD4^+CD25^-IL17^+$ Th17 cells were relevant to IBD and asthma. In IBD, Th17 cells are proinflammatory by secreting cytokines, recruitment of neutrophils, or transformation into Th1 cells [49]. In asthma, Th17 cytokines, such as IL-17A and IL-22, can promote neutrophil recruitment in the airways and are involved in airway remodeling and hyperresponsiveness via binding to IL-17RA and IL-17RC in airway smooth muscle cells [50]. Drugs have been developed to treat IBD and asthma by targeting Th17 cells. For example, ustekinumab targeting Th17 differentiation has been used to treat IBD, and secukinumab targeting IL-17A is in phase II clinical trials for treating asthma (NCT01478360). Consistent with our results, a recent study has reported that abnormal humoral immunity mediated by Th17 cells may be a pathogenic mechanism shared by IgAN and IBD [51]. Given the potential shared immunopathogenesis related to Th17 cells, treatment targeting the imbalance of the T cells compartment may be desirable for IgAN.

Based on a limited number of significant IgAN GWAS loci, previous studies have reported shared pleiotropic loci between IgAN and many other complex traits and diseases [8]. By contrast, we performed GPA pleiotropy analysis based on GWAS summary statistics across the whole genome. Three novel loci (i.e., *PNKD*, *UBE2L3*, and *SCAF8*) of 11 loci showing pleiotropic effect between IgAN and IBD and between IgAN and asthma were identified by pleiotropic analyses. Notably, two pleiotropic loci between IgAN and asthma, namely, S*CAF8* and *OVOL1*, were not associated with asthma in the GWAS we used. However, they have been reported to significantly associate with asthma in a recent study with a larger sample size [52], which supports the validity and effectiveness of the integrative analysis approach we used. Among the pleiotropic loci, *UBE2L3* and *ZMIZ1* have pleiotropic effects on IgAN and IBD. *UBE2L3* encodes a member of the E2 ubiquitin-conjugating enzyme family, which is involved in ubiquitin/proteasome-dependent degradation. The ubiquitin/proteasome pathway has been implicated in the development of multiple kidney diseases [53]. Proteasome inhibitors, such as bortezomib, have been efficacious in some renal disorders [54–56]. Moreover, elevated expression and activity of UBE2L3 might trigger autoimmune diseases by altering immune response pathways, such as the nuclear transcription factor κB signaling pathway, GSK3b/p65 signaling pathway, and p53 signaling pathway [53]. *ZMIZ1* encodes a member of the PIAS (protein inhibitor of activated STAT) family of proteins, which play critical roles in the immune system by influencing T cell development and regulating TGF-β/Smad pathway [57]. In fact, genetic variants in *UBE2L3* and *ZMIZ1* have been reported to associate with several immune or inflammatory disease [58–60]. The GWAS of IgAN by Kiryluk *et al.* has also reported *ZMIZ1* and *OVOL1* as the novel loci of IgAN, which provided evidence to support our results [11]. These pleiotropic analysis results, together with the cell-type specific analysis, highlight the involvement of IL-17 signal pathway and T cell immunity in the pathophysiology of IgAN.

Besides pleiotropic loci, our integrative analyses identified three other novel loci at 14q32.32, 16q22.2, and 21q21.3 with specific associations with IgAN, potentially due to gain in statistical power by incorporating functional annotations. Notably, *TRAF3* at 14q32.32 encodes a TNF receptor-associated factor that participates in the signal transduction of CD40 and in the regulation of T cell dependent immune responses and antiviral responses [61]. Genetic variants in *TRAF3* have been reported to associate with hematological traits [62], serum IgA level [63], and asthma [64]. The two other loci, namely, *TXNL4B* at 16q22.2 and *LINC00113* at 21q21.3,

are not directly related to immune functions. By contrast, they have been reported to associate with cardiovascular disease [65], type 2 diabetes [66], and chronic renal failure [67].

In conclusion, through comprehensive GWAS meta-analysis and post-GWAS enrichment and integrative analysis, we have pinpointed PMA-I-stimulated $CD4^+CD25^-IL17^+$ Th17 cells as the most relevant cell type for IgAN and identified seven novel and biologically relevant loci in association with IgAN (Table 3). However, some limitations of our study should be considered. First, we did not conduct replication analysis or experimental validation of the novel loci, despite their important roles in T cell immune response and inflammation. In the future, we will conduct further validation through another large independent population. Second, the GWAS summary statistics of IBD and asthma were based on European populations while the IgAN GWASs were based on Chinese population. Although using GWASs from the same population is ideal for GPA analysis, we suggest that most of the underlying causal variants are shared across populations, as demonstrated by several recent multi-ethnic GWASs of complex diseases [68]. Third, the identification analysis of cell types relevant to specific traits may be restricted by the functional annotations of available tissues and cell types, although multiple immune cell types have been explored in our study. Moreover, we have pruned the variants to be approximately independent in the GPA analysis to minimize the effect of LD difference across populations. Despite these limitations, our findings highlight the involvement of T cell immunity, especially Th17 cells, in the development of IgAN. Our results also provide critical information for future functional studies to advance understanding of the etiology of IgAN.

Acknowledgements

We are grateful to all the subjects and healthy volunteers who participated in this work. We thank Professor Jianjun Liu for reviewing the article and providing constructive suggestions. This work was supported by Guangdong–Hong Kong Joint Laboratory on Immunological and Genetic Kidney Diseases (No. 2019B121205005), National Natural Science Foundation of China (Nos. 81920108008, 81770661, 82170714, and 82003561), Guangzhou Municipal Science and Technology Project of China (No. 202201011246), Basic and Applied Basic Research Foundation of Guangdong Province (No. 2021A1515111054) and Fundamental Research Funds for the Central Universities (No. 2019kfyXJJS036).

Compliance with ethics guidelines

Conflicts of interest Ming Li , Xingjie Hao, Dianchun Shi, Shanshan Cheng, Zhong Zhong, Lu Cai, Minghui Jiang, Lin Ding, Lanbo Ding, Chaolong Wang, and Xueqing Yu declare that they have no conflict of interest.

The study was approved by the Institutional Review Board at the Guangdong Provincial People's Hospital (No. GDREC2019272H) and the First Affiliated Hospital of Sun Yat-sen University (No. 2016215) according to the Declaration of Helsinki and the study was performed in accordance with the ethical standards as laid down in the 1964 Declaration of Helsinki and its later amendments or comparable ethical standards. Informed consent was obtained from all patients for being included in the study.

Electronic Supplementary Material Supplementary material is available in the online version of this article at https://doi.org/10.1007/s11684-024-1086-2 and is accessible for authorized users.

References

1. Zhang H, Barratt J. Is IgA nephropathy the same disease in different parts of the world? Semin Immunopathol 2021; 43(5): 707–715
2. Coppo R, Amore A, Hogg R, Emancipator S. Idiopathic nephropathy with IgA deposits. Pediatr Nephrol 2000; 15(1–2): 139–150
3. Magistroni R, D'Agati VD, Appel GB, Kiryluk K. New developments in the genetics, pathogenesis, and therapy of IgA nephropathy. Kidney Int 2015; 88(5): 974–989
4. Schena FP, Nistor I. Epidemiology of IgA nephropathy: a global perspective. Semin Nephrol 2018; 38(5): 435–442
5. Li M, Wang L, Shi DC, Foo JN, Zhong Z, Khor CC, Lanzani C, Citterio L, Salvi E, Yin PR, Bei JX, Wang L, Liao YH, Chen J, Chen QK, Xu G, Jiang GR, Wan JX, Chen MH, Chen N, Zhang H, Zeng YX, Liu ZH, Liu JJ, Yu XQ. Genome-wide meta-analysis identifies three novel susceptibility loci and reveals ethnic heterogeneity of genetic susceptibility for IgA nephropathy. J Am Soc Nephrol 2020; 31(12): 2949–2963
6. Feehally J, Farrall M, Boland A, Gale DP, Gut I, Heath S, Kumar A, Peden JF, Maxwell PH, Morris DL, Padmanabhan S, Vyse TJ, Zawadzka A, Rees AJ, Lathrop M, Ratcliffe PJ. HLA has strongest association with IgA nephropathy in genome-wide analysis. J Am Soc Nephrol 2010; 21(10): 1791–1797
7. Yu XQ, Li M, Zhang H, Low HQ, Wei X, Wang JQ, Sun LD, Sim KS, Li Y, Foo JN, Wang W, Li ZJ, Yin XY, Tang XQ, Fan L, Chen J, Li RS, Wan JX, Liu ZS, Lou TQ, Zhu L, Huang XJ, Zhang XJ, Liu ZH, Liu JJ. A genome-wide association study in Han Chinese identifies multiple susceptibility loci for IgA nephropathy. Nat Genet 2012; 44(2): 178–182
8. Kiryluk K, Li Y, Scolari F, Sanna-Cherchi S, Choi M, Verbitsky M, Fasel D, Lata S, Prakash S, Shapiro S, Fischman C, Snyder HJ, Appel G, Izzi C, Viola BF, Dallera N, Del Vecchio L, Barlassina C, Salvi E, Bertinetto FE, Amoroso A, Savoldi S, Rocchietti M, Amore A, Peruzzi L, Coppo R, Salvadori M, Ravani P, Magistroni R, Ghiggeri GM, Caridi G, Bodria M, Lugani F, Allegri L, Delsante M, Maiorana M, Magnano A, Frasca G, Boer E, Boscutti G, Ponticelli C, Mignani R, Marcantoni C, Di Landro D, Santoro D, Pani A, Polci R, Feriozzi S, Chicca S, Galliani M, Gigante M, Gesualdo L, Zamboli P, Battaglia GG, Garozzo M, Maixnerová D,

Tesar V, Eitner F, Rauen T, Floege J, Kovacs T, Nagy J, Mucha K, Pączek L, Zaniew M, Mizerska-Wasiak M, Roszkowska-Blaim M, Pawlaczyk K, Gale D, Barratt J, Thibaudin L, Berthoux F, Canaud G, Boland A, Metzger M, Panzer U, Suzuki H, Goto S, Narita I, Caliskan Y, Xie J, Hou P, Chen N, Zhang H, Wyatt RJ, Novak J, Julian BA, Feehally J, Stengel B, Cusi D, Lifton RP, Gharavi AG. Discovery of new risk loci for IgA nephropathy implicates genes involved in immunity against intestinal pathogens. Nat Genet 2014; 46(11): 1187–1196

9. Li M, Foo JN, Wang JQ, Low HQ, Tang XQ, Toh KY, Yin PR, Khor CC, Goh YF, Irwan ID, Xu RC, Andiappan AK, Bei JX, Rotzschke O, Chen MH, Cheng CY, Sun LD, Jiang GR, Wong TY, Lin HL, Aung T, Liao YH, Saw SM, Ye K, Ebstein RP, Chen QK, Shi W, Chew SH, Chen J, Zhang FR, Li SP, Xu G, Shyong Tai E, Wang L, Chen N, Zhang XJ, Zeng YX, Zhang H, Liu ZH, Yu XQ, Liu JJ. Identification of new susceptibility loci for IgA nephropathy in Han Chinese. Nat Commun 2015; 6(1): 7270
10. Gharavi AG, Kiryluk K, Choi M, Li Y, Hou P, Xie J, Sanna-Cherchi S, Men CJ, Julian BA, Wyatt RJ, Novak J, He JC, Wang H, Lv J, Zhu L, Wang W, Wang Z, Yasuno K, Gunel M, Mane S, Umlauf S, Tikhonova I, Beerman I, Savoldi S, Magistroni R, Ghiggeri GM, Bodria M, Lugani F, Ravani P, Ponticelli C, Allegri L, Boscutti G, Frasca G, Amore A, Peruzzi L, Coppo R, Izzi C, Viola BF, Prati E, Salvadori M, Mignani R, Gesualdo L, Bertinetto F, Mesiano P, Amoroso A, Scolari F, Chen N, Zhang H, Lifton RP. Genome-wide association study identifies susceptibility loci for IgA nephropathy. Nat Genet 2011; 43(4): 321–327
11. Kiryluk K, Sanchez-Rodriguez E, Zhou XJ, Zanoni F, Liu L, Mladkova N, Khan A, Marasa M, Zhang JY, Balderes O, Sanna-Cherchi S, Bomback AS, Canetta PA, Appel GB, Radhakrishnan J, Trimarchi H, Sprangers B, Cattran DC, Reich H, Pei Y, Ravani P, Galesic K, Maixnerova D, Tesar V, Stengel B, Metzger M, Canaud G, Maillard N, Berthoux F, Berthelot L, Pillebout E, Monteiro R, Nelson R, Wyatt RJ, Smoyer W, Mahan J, Samhar AA, Hidalgo G, Quiroga A, Weng P, Sreedharan R, Selewski D, Davis K, Kallash M, Vasylyeva TL, Rheault M, Chishti A, Ranch D, Wenderfer SE, Samsonov D, Claes DJ, Akchurin O, Goumenos D, Stangou M, Nagy J, Kovacs T, Fiaccadori E, Amoroso A, Barlassina C, Cusi D, Del Vecchio L, Battaglia GG, Bodria M, Boer E, Bono L, Boscutti G, Caridi G, Lugani F, Ghiggeri G, Coppo R, Peruzzi L, Esposito V, Esposito C, Feriozzi S, Polci R, Frasca G, Galliani M, Garozzo M, Mitrotti A, Gesualdo L, Granata S, Zaza G, Londrino F, Magistroni R, Pisani I, Magnano A, Marcantoni C, Messa P, Mignani R, Pani A, Ponticelli C, Roccatello D, Salvadori M, Salvi E, Santoro D, Gembillo G, Savoldi S, Spotti D, Zamboli P, Izzi C, Alberici F, Delbarba E, Florczak M, Krata N, Mucha K, Pączek L, Niemczyk S, Moszczuk B, Pańczyk-Tomaszewska M, Mizerska-Wasiak M, Perkowska-Ptasińska A, Bączkowska T, Durlik M, Pawlaczyk K, Sikora P, Zaniew M, Kaminska D, Krajewska M, Kuzmiuk-Glembin I, Heleniak Z, Bullo-Piontecka B, Liberek T, Dębska-Slizien A, Hryszko T, Materna-Kiryluk A, Miklaszewska M, Szczepańska M, Dyga K, Machura E, Siniewicz-Luzeńczyk K, Pawlak-Bratkowska M, Tkaczyk M, Runowski D, Kwella N, Drożdż D, Habura I, Kronenberg F, Prikhodina L, van Heel D, Fontaine B, Cotsapas C, Wijmenga C, Franke A, Annese V, Gregersen PK, Parameswaran S, Weirauch M, Kottyan L, Harley JB, Suzuki H, Narita I, Goto S, Lee H, Kim DK, Kim YS, Park JH, Cho B, Choi M, Van Wijk A, Huerta A, Ars E, Ballarin J, Lundberg S, Vogt B, Mani LY, Caliskan Y, Barratt J, Abeygunaratne T, Kalra PA, Gale DP, Panzer U, Rauen T, Floege J, Schlosser P, Ekici AB, Eckardt KU, Chen N, Xie J, Lifton RP, Loos RJF, Kenny EE, Ionita-Laza I, Köttgen A, Julian BA, Novak J, Scolari F, Zhang H, Gharavi AG. Genome-wide association analyses define pathogenic signaling pathways and prioritize drug targets for IgA nephropathy. Nat Genet 2023; 55(7): 1091–1105
12. Shi D, Zhong Z, Wang M, Cai L, Fu D, Peng Y, Guo L, Mao H, Yu X, Li M. Identification of susceptibility locus shared by IgA nephropathy and inflammatory bowel disease in a Chinese Han population. J Hum Genet 2020; 65(3): 241–249
13. Floege J, Feehally J. The mucosa-kidney axis in IgA nephropathy. Nat Rev Nephrol 2016; 12(3): 147–156
14. Gesualdo L, Di Leo V, Coppo R. The mucosal immune system and IgA nephropathy. Semin Immunopathol 2021; 43(5): 657–668
15. Cheung CK, Barratt J. Further evidence for the mucosal origin of pathogenic IgA in IgA nephropathy. J Am Soc Nephrol 2022; 33(5): 873–875
16. Fellström BC, Barratt J, Cook H, Coppo R, Feehally J, de Fijter JW, Floege J, Hetzel G, Jardine AG, Locatelli F, Maes BD, Mercer A, Ortiz F, Praga M, Sørensen SS, Tesar V, Del Vecchio L; NEFIGAN Trial Investigators. Targeted-release budesonide versus placebo in patients with IgA nephropathy (NEFIGAN): a double-blind, randomised, placebo-controlled phase 2b trial. Lancet 2017; 389(10084): 2117–2127
17. Chung D, Yang C, Li C, Gelernter J, Zhao H. GPA: a statistical approach to prioritizing GWAS results by integrating pleiotropy and annotation. PLoS Genet 2014; 10(11): e1004787
18. Liu JZ, van Sommeren S, Huang H, Ng SC, Alberts R, Takahashi A, Ripke S, Lee JC, Jostins L, Shah T, Abedian S, Cheon JH, Cho J, Dayani NE, Franke L, Fuyuno Y, Hart A, Juyal RC, Juyal G, Kim WH, Morris AP, Poustchi H, Newman WG, Midha V, Orchard TR, Vahedi H, Sood A, Sung JY, Malekzadeh R, Westra HJ, Yamazaki K, Yang SK; International Multiple Sclerosis Genetics Consortium; International IBD Genetics Consortium; Barrett JC, Alizadeh BZ, Parkes M, Bk T, Daly MJ, Kubo M, Anderson CA, Weersma RK. Association analyses identify 38 susceptibility loci for inflammatory bowel disease and highlight shared genetic risk across populations. Nat Genet 2015; 47(9): 979–986
19. Zhu Z, Lee PH, Chaffin MD, Chung W, Loh PR, Lu Q, Christiani DC, Liang L. A genome-wide cross-trait analysis from UK Biobank highlights the shared genetic architecture of asthma and allergic diseases. Nat Genet 2018; 50(6): 857–864
20. Wu D, Dou J, Chai X, Bellis C, Wilm A, Shih CC, Soon WWJ, Bertin N, Lin CB, Khor CC, DeGiorgio M, Cheng S, Bao L, Karnani N, Hwang WYK, Davila S, Tan P, Shabbir A, Moh A, Tan EK, Foo JN, Goh LL, Leong KP, Foo RSY, Lam CSP, Richards AM, Cheng CY, Aung T, Wong TY, Ng HH; SG10K Consortium; Liu J, Wang C. Large-scale whole-genome sequencing of three diverse Asian populations in Singapore. Cell 2019; 179(3): 736–749.e15
21. Chang CC, Chow CC, Tellier LC, Vattikuti S, Purcell SM, Lee JJ. Second-generation PLINK: rising to the challenge of larger and richer datasets. Gigascience 2015; 4(1): 7
22. 1000 Genomes Project Consortium; Auton A, Brooks LD, Durbin RM, Garrison EP, Kang HM, Korbel JO, Marchini JL, McCarthy S, McVean GA, Abecasis GR. A global reference for human

genetic variation. Nature 2015; 526(7571): 68–74
23. Loh PR, Danecek P, Palamara PF, Fuchsberger C, Reshef YA, Finucane HK, Schoenherr S, Forer L, McCarthy S, Abecasis GR, Durbin R, Price AL. Reference-based phasing using the Haplotype Reference Consortium panel. Nat Genet 2016; 48(11): 1443–1448
24. Das S, Forer L, Schönherr S, Sidore C, Locke AE, Kwong A, Vrieze SI, Chew EY, Levy S, McGue M, Schlessinger D, Stambolian D, Loh PR, Iacono WG, Swaroop A, Scott LJ, Cucca F, Kronenberg F, Boehnke M, Abecasis GR, Fuchsberger C. Next-generation genotype imputation service and methods. Nat Genet 2016; 48(10): 1284–1287
25. Danecek P, Bonfield JK, Liddle J, Marshall J, Ohan V, Pollard MO, Whitwham A, Keane T, McCarthy SA, Davies RM, Li H. Twelve years of SAMtools and BCFtools. Gigascience 2021; 10(2): giab008
26. Willer CJ, Li Y, Abecasis GR. METAL: fast and efficient meta-analysis of genomewide association scans. Bioinformatics 2010; 26(17): 2190–2191
27. Bulik-Sullivan BK, Loh PR, Finucane HK, Ripke S, Yang J; Schizophrenia Working Group of the Psychiatric Genomics Consortium; Patterson N, Daly MJ, Price AL, Neale BM. LD score regression distinguishes confounding from polygenicity in genome-wide association studies. Nat Genet 2015; 47(3): 291–295
28. Watanabe K, Taskesen E, van Bochoven A, Posthuma D. Functional mapping and annotation of genetic associations with FUMA. Nat Commun 2017; 8(1): 1826
29. GTEx Consortium. The Genotype-Tissue Expression (GTEx) pilot analysis: multitissue gene regulation in humans. Science 2015; 348(6235): 648–660
30. Lu Q, Powles RL, Abdallah S, Ou D, Wang Q, Hu Y, Lu Y, Liu W, Li B, Mukherjee S, Crane PK, Zhao H. Systematic tissue-specific functional annotation of the human genome highlights immune-related DNA elements for late-onset Alzheimer's disease. PLoS Genet 2017; 13(7): e1006933
31. Finucane HK, Bulik-Sullivan B, Gusev A, Trynka G, Reshef Y, Loh PR, Anttila V, Xu H, Zang C, Farh K, Ripke S, Day FR; ReproGen Consortium; Schizophrenia Working Group of the Psychiatric Genomics Consortium; RACI Consortium; Purcell S, Stahl E, Lindstrom S, Perry JR, Okada Y, Raychaudhuri S, Daly MJ, Patterson N, Neale BM, Price AL. Partitioning heritability by functional annotation using genome-wide association summary statistics. Nat Genet 2015; 47(11): 1228–1235
32. Roadmap Epigenomics Consortium; Kundaje A, Meuleman W, Ernst J, Bilenky M, Yen A, Heravi-Moussavi A, Kheradpour P, Zhang Z, Wang J, Ziller MJ, Amin V, Whitaker JW, Schultz MD, Ward LD, Sarkar A, Quon G, Sandstrom RS, Eaton ML, Wu YC, Pfenning AR, Wang X, Claussnitzer M, Liu Y, Coarfa C, Harris RA, Shoresh N, Epstein CB, Gjoneska E, Leung D, Xie W, Hawkins RD, Lister R, Hong C, Gascard P, Mungall AJ, Moore R, Chuah E, Tam A, Canfield TK, Hansen RS, Kaul R, Sabo PJ, Bansal MS, Carles A, Dixon JR, Farh KH, Feizi S, Karlic R, Kim AR, Kulkarni A, Li D, Lowdon R, Elliott G, Mercer TR, Neph SJ, Onuchic V, Polak P, Rajagopal N, Ray P, Sallari RC, Siebenthall KT, Sinnott-Armstrong NA, Stevens M, Thurman RE, Wu J, Zhang B, Zhou X, Beaudet AE, Boyer LA, De Jager PL, Farnham PJ, Fisher SJ, Haussler D, Jones SJ, Li W, Marra MA, McManus MT, Sunyaev S, Thomson JA, Tlsty TD, Tsai LH, Wang W, Waterland RA, Zhang MQ, Chadwick LH, Bernstein BE, Costello JF, Ecker JR, Hirst M, Meissner A, Milosavljevic A, Ren B, Stamatoyannopoulos JA, Wang T, Kellis M. Integrative analysis of 111 reference human epigenomes. Nature 2015; 518(7539): 317–330
33. Giambartolomei C, Vukcevic D, Schadt EE, Franke L, Hingorani AD, Wallace C, Plagnol V. Bayesian test for colocalisation between pairs of genetic association studies using summary statistics. PLoS Genet 2014; 10(5): e1004383
34. Liu B, Gloudemans MJ, Rao AS, Ingelsson E, Montgomery SB. Abundant associations with gene expression complicate GWAS follow-up. Nat Genet 2019; 51(5): 768–769
35. Adzhubei IA, Schmidt S, Peshkin L, Ramensky VE, Gerasimova A, Bork P, Kondrashov AS, Sunyaev SR. A method and server for predicting damaging missense mutations. Nat Methods 2010; 7(4): 248–249
36. Sim NL, Kumar P, Hu J, Henikoff S, Schneider G, Ng PC. SIFT web server: predicting effects of amino acid substitutions on proteins. Nucleic Acids Res 2012; 40(Web Server issue): W452–457
37. GTEx Consortium. The genotype-tissue expression (GTEx) project. Nat Genet 2013; 45(6): 580–585
38. Fanucchi S, Fok ET, Dalla E, Shibayama Y, Börner K, Chang EY, Stoychev S, Imakaev M, Grimm D, Wang KC, Li G, Sung WK, Mhlanga MM. Immune genes are primed for robust transcription by proximal long noncoding RNAs located in nuclear compartments. Nat Genet 2019; 51(1): 138–150
39. He B, Chen C, Teng L, Tan K. Global view of enhancer-promoter interactome in human cells. Proc Natl Acad Sci USA 2014; 111(21): E2191–E2199
40. Ahmad Mokhtar AM, Hashim IF, Mohd Zaini Makhtar M, Salikin NH, Amin-Nordin S. The role of RhoH in TCR signalling and its involvement in diseases. Cells 2021; 10(4): 950
41. Tamehiro N, Nishida K, Sugita Y, Hayakawa K, Oda H, Nitta T, Nakano M, Nishioka A, Yanobu-Takanashi R, Goto M, Okamura T, Adachi R, Kondo K, Morita A, Suzuki H. Ras homolog gene family H (RhoH) deficiency induces psoriasis-like chronic dermatitis by promoting T_H17 cell polarization. J Allergy Clin Immunol 2019; 143(5): 1878–1891
42. Tang Y, He H, Hu P, Xu X. T lymphocytes in IgA nephropathy. Exp Ther Med 2020; 20(1): 186–194
43. Schmidt T, Luebbe J, Kilian C, Riedel JH, Hiekmann S, Asada N, Ginsberg P, Robben L, Song N, Kaffke A, Peters A, Borchers A, Flavell RA, Gagliani N, Pelzcar P, Huber S, Huber TB, Turner JE, Paust HJ, Krebs CF, Panzer U. IL-17 receptor C signaling controls $CD4^+$ T_H17 immune responses and tissue injury in immune-mediated kidney diseases. J Am Soc Nephrol 2021; 32(12): 3081–3098
44. Ruszkowski J, Lisowska KA, Pindel M, Heleniak Z, Dębska-Ślizień A, Witkowski JM. T cells in IgA nephropathy: role in pathogenesis, clinical significance and potential therapeutic target. Clin Exp Nephrol 2019; 23(3): 291–303
45. Yang L, Zhang X, Peng W, Wei M, Qin W. MicroRNA-155-induced T lymphocyte subgroup drifting in IgA nephropathy. Int Urol Nephrol 2017; 49(2): 353–361
46. Du W, Gao CY, You X, Li L, Zhao ZB, Fang M, Ye Z, Si M, Lian ZX, Yu X. Increased proportion of follicular helper T cells is associated with B cell activation and disease severity in IgA nephropathy. Front Immunol 2022; 13: 901465

47. Lin FJ, Jiang GR, Shan JP, Zhu C, Zou J, Wu XR. Imbalance of regulatory T cells to Th17 cells in IgA nephropathy. Scand J Clin Lab Invest 2012; 72(3): 221–229
48. Lin JR, Wen J, Zhang H, Wang L, Gou FF, Yang M, Fan JM. Interleukin-17 promotes the production of underglycosylated IgA1 in DAKIKI cells. Ren Fail 2018; 40(1): 60–67
49. Jiang P, Zheng C, Xiang Y, Malik S, Su D, Xu G, Zhang M. The involvement of TH17 cells in the pathogenesis of IBD. Cytokine Growth Factor Rev 2023; 69: 28–42
50. Jeong J, Lee HK. The role of $CD4^+$ T cells and microbiota in the pathogenesis of asthma. Int J Mol Sci 2021; 22(21): 11822
51. Qing J, Li C, Hu X, Song W, Tirichen H, Yaigoub H, Li Y. Differentiation of T helper 17 cells may mediate the abnormal humoral immunity in IgA nephropathy and inflammatory bowel disease based on shared genetic effects. Front Immunol 2022; 13: 916934
52. Han Y, Jia Q, Jahani PS, Hurrell BP, Pan C, Huang P, Gukasyan J, Woodward NC, Eskin E, Gilliland FD, Akbari O, Hartiala JA, Allayee H. Genome-wide analysis highlights contribution of immune system pathways to the genetic architecture of asthma. Nat Commun 2020; 11(1): 1776
53. Zhang X, Huo C, Liu Y, Su R, Zhao Y, Li Y. Mechanism and disease association with a ubiquitin conjugating E2 enzyme: UBE2L3. Front Immunol 2022; 13: 793610
54. Lechner SM, Abbad L, Boedec E, Papista C, Le Stang MB, Moal C, Maillard J, Jamin A, Bex-Coudrat J, Wang Y, Li A, Martini PG, Monteiro RC, Berthelot L. IgA1 protease treatment reverses mesangial deposits and hematuria in a model of IgA nephropathy. J Am Soc Nephrol 2016; 27(9): 2622–2629
55. Neubert K, Meister S, Moser K, Weisel F, Maseda D, Amann K, Wiethe C, Winkler TH, Kalden JR, Manz RA, Voll RE. The proteasome inhibitor bortezomib depletes plasma cells and protects mice with lupus-like disease from nephritis. Nat Med 2008; 14(7): 748–755
56. Bontscho J, Schreiber A, Manz RA, Schneider W, Luft FC, Kettritz R. Myeloperoxidase-specific plasma cell depletion by bortezomib protects from anti-neutrophil cytoplasmic autoantibodies-induced glomerulonephritis. J Am Soc Nephrol 2011; 22(2): 336–348
57. Wan YY, Flavell RA. TGF-beta and regulatory T cell in immunity and autoimmunity. J Clin Immunol 2008; 28(6): 647–659
58. International Genetics of Ankylosing Spondylitis Consortium (IGAS); Cortes A, Hadler J, Pointon JP, Robinson PC, Karaderi T, Leo P, Cremin K, Pryce K, Harris J, Lee S, Joo KB, Shim SC, Weisman M, Ward M, Zhou X, Garchon HJ, Chiocchia G, Nossent J, Lie BA, Førre Ø, Tuomilehto J, Laiho K, Jiang L, Liu Y, Wu X, Bradbury LA, Elewaut D, Burgos-Vargas R, Stebbings S, Appleton L, Farrah C, Lau J, Kenna TJ, Haroon N, Ferreira MA, Yang J, Mulero J, Fernandez-Sueiro JL, Gonzalez-Gay MA, Lopez-Larrea C, Deloukas P, Donnelly P; Australo-Anglo-American Spondyloarthritis Consortium (TASC); Groupe Française d'Etude Génétique des Spondylarthrites (GFEGS); Nord-Trøndelag Health Study (HUNT); Spondyloarthritis Research Consortium of Canada (SPARCC); Wellcome Trust Case Control Consortium 2 (WTCCC2); Bowness P, Gafney K, Gaston H, Gladman DD, Rahman P, Maksymowych WP, Xu H, Crusius JB, van der Horst-Bruinsma IE, Chou CT, Valle-Oñate R, Romero-Sánchez C, Hansen IM, Pimentel-Santos FM, Inman RD, Videm V, Martin J, Breban M, Reveille JD, Evans DM, Kim TH, Wordsworth BP, Brown MA. Identification of multiple risk variants for ankylosing spondylitis through high-density genotyping of immune-related loci. Nat Genet 2013; 45(7): 730–738
59. Langefeld CD, Ainsworth HC, Cunninghame Graham DS, Kelly JA, Comeau ME, Marion MC, Howard TD, Ramos PS, Croker JA, Morris DL, Sandling JK, Almlöf JC, Acevedo-Vásquez EM, Alarcón GS, Babini AM, Baca V, Bengtsson AA, Berbotto GA, Bijl M, Brown EE, Brunner HI, Cardiel MH, Catoggio L, Cervera R, Cucho-Venegas JM, Dahlqvist SR, D'Alfonso S, Da Silva BM, de la Rúa Figueroa I, Doria A, Edberg JC, Endreffy E, Esquivel-Valerio JA, Fortin PR, Freedman BI, Frostegård J, García MA, de la Torre IG, Gilkeson GS, Gladman DD, Gunnarsson I, Guthridge JM, Huggins JL, James JA, Kallenberg CGM, Kamen DL, Karp DR, Kaufman KM, Kottyan LC, Kovács L, Laustrup H, Lauwerys BR, Li QZ, Maradiaga-Ceceña MA, Martín J, McCune JM, McWilliams DR, Merrill JT, Miranda P, Moctezuma JF, Nath SK, Niewold TB, Orozco L, Ortego-Centeno N, Petri M, Pineau CA, Pons-Estel BA, Pope J, Raj P, Ramsey-Goldman R, Reveille JD, Russell LP, Sabio JM, Aguilar-Salinas CA, Scherbarth HR, Scorza R, Seldin MF, Sjöwall C, Svenungsson E, Thompson SD, Toloza SMA, Truedsson L, Tusié-Luna T, Vasconcelos C, Vilá LM, Wallace DJ, Weisman MH, Wither JE, Bhangale T, Oksenberg JR, Rioux JD, Gregersen PK, Syvänen AC, Rönnblom L, Criswell LA, Jacob CO, Sivils KL, Tsao BP, Schanberg LE, Behrens TW, Silverman ED, Alarcón-Riquelme ME, Kimberly RP, Harley JB, Wakeland EK, Graham RR, Gaffney PM, Vyse TJ. Transancestral mapping and genetic load in systemic lupus erythematosus. Nat Commun 2017; 8(1): 16021
60. Kim K, Bang SY, Lee HS, Cho SK, Choi CB, Sung YK, Kim TH, Jun JB, Yoo DH, Kang YM, Kim SK, Suh CH, Shim SC, Lee SS, Lee J, Chung WT, Choe JY, Shin HD, Lee JY, Han BG, Nath SK, Eyre S, Bowes J, Pappas DA, Kremer JM, Gonzalez-Gay MA, Rodriguez-Rodriguez L, Ärlestig L, Okada Y, Diogo D, Liao KP, Karlson EW, Raychaudhuri S, Rantapää-Dahlqvist S, Martin J, Klareskog L, Padyukov L, Gregersen PK, Worthington J, Greenberg JD, Plenge RM, Bae SC. High-density genotyping of immune loci in Koreans and Europeans identifies eight new rheumatoid arthritis risk loci. Ann Rheum Dis 2015; 74(3): e13
61. Li H, Hostager BS, Arkee T, Bishop GA. Multiple mechanisms for TRAF3-mediated regulation of the T cell costimulatory receptor GITR. J Biol Chem 2021; 297(3): 101097
62. Astle WJ, Elding H, Jiang T, Allen D, Ruklisa D, Mann AL, Mead D, Bouman H, Riveros-Mckay F, Kostadima MA, Lambourne JJ, Sivapalaratnam S, Downes K, Kundu K, Bomba L, Berentsen K, Bradley JR, Daugherty LC, Delaneau O, Freson K, Garner SF, Grassi L, Guerrero J, Haimel M, Janssen-Megens EM, Kaan A, Kamat M, Kim B, Mandoli A, Marchini J, Martens JHA, Meacham S, Megy K, O'Connell J, Petersen R, Sharifi N, Sheard SM, Staley JR, Tuna S, van der Ent M, Walter K, Wang SY, Wheeler E, Wilder SP, Iotchkova V, Moore C, Sambrook J, Stunnenberg HG, Di Angelantonio E, Kaptoge S, Kuijpers TW, Carrillo-de-Santa-Pau E, Juan D, Rico D, Valencia A, Chen L, Ge B, Vasquez L, Kwan T, Garrido-Martín D, Watt S, Yang Y, Guigo R, Beck S, Paul DS, Pastinen T, Bujold D, Bourque G, Frontini M, Danesh J, Roberts DJ, Ouwehand WH, Butterworth AS, Soranzo N. The allelic landscape of human blood cell trait variation and links to

common complex disease. Cell 2016; 167(5): 1415–1429.e19
63. Jonsson S, Sveinbjornsson G, de Lapuente Portilla AL, Swaminathan B, Plomp R, Dekkers G, Ajore R, Ali M, Bentlage AEH, Elmér E, Eyjolfsson GI, Gudjonsson SA, Gullberg U, Gylfason A, Halldorsson BV, Hansson M, Holm H, Johansson Å, Johnsson E, Jonasdottir A, Ludviksson BR, Oddsson A, Olafsson I, Olafsson S, Sigurdardottir O, Sigurdsson A, Stefansdottir L, Masson G, Sulem P, Wuhrer M, Wihlborg AK, Thorleifsson G, Gudbjartsson DF, Thorsteinsdottir U, Vidarsson G, Jonsdottir I, Nilsson B, Stefansson K. Identification of sequence variants influencing immunoglobulin levels. Nat Genet 2017; 49(8): 1182–1191
64. Johansson Å, Rask-Andersen M, Karlsson T, Ek WE. Genome-wide association analysis of 350 000 Caucasians from the UK Biobank identifies novel loci for asthma, hay fever and eczema. Hum Mol Genet 2019; 28(23): 4022–4041
65. van der Harst P, Verweij N. Identification of 64 novel genetic loci provides an expanded view on the genetic architecture of coronary artery disease. Circ Res 2018; 122(3): 433–443
66. Vujkovic M, Keaton JM, Lynch JA, Miller DR, Zhou J, Tcheandjieu C, Huffman JE, Assimes TL, Lorenz K, Zhu X, Hilliard AT, Judy RL, Huang J, Lee KM, Klarin D, Pyarajan S, Danesh J, Melander O, Rasheed A, Mallick NH, Hameed S, Qureshi IH, Afzal MN, Malik U, Jalal A, Abbas S, Sheng X, Gao L, Kaestner KH, Susztak K, Sun YV, DuVall SL, Cho K, Lee JS, Gaziano JM, Phillips LS, Meigs JB, Reaven PD, Wilson PW, Edwards TL, Rader DJ, Damrauer SM, O'Donnell CJ, Tsao PS; HPAP Consortium; Regeneron Genetics Center; VA Million Veteran Program; Chang KM, Voight BF, Saleheen D. Discovery of 318 new risk loci for type 2 diabetes and related vascular outcomes among 1.4 million participants in a multi-ancestry meta-analysis. Nat Genet 2020; 52(7): 680–691
67. Murea M, Lu L, Ma L, Hicks PJ, Divers J, McDonough CW, Langefeld CD, Bowden DW, Freedman BI. Genome-wide association scan for survival on dialysis in African-Americans with type 2 diabetes. Am J Nephrol 2011; 33(6): 502–509
68. Marigorta UM, Navarro A. High trans-ethnic replicability of GWAS results implies common causal variants. PLoS Genet 2013; 9(6): e1003566
69. Orlando G, Law PJ, Palin K, Tuupanen S, Gylfe A, Hänninen UA, Cajuso T, Tanskanen T, Kondelin J, Kaasinen E, Sarin AP, Kaprio J, Eriksson JG, Rissanen H, Knekt P, Pukkala E, Jousilahti P, Salomaa V, Ripatti S, Palotie A, Järvinen H, Renkonen-Sinisalo L, Lepistö A, Böhm J, Mecklin JP, Al-Tassan NA, Palles C, Martin L, Barclay E, Tenesa A, Farrington S, Timofeeva MN, Meyer BF, Wakil SM, Campbell H, Smith CG, Idziaszczyk S, Maughan TS, Kaplan R, Kerr R, Kerr D, Buchanan DD, Win AK, Hopper J, Jenkins M, Lindor NM, Newcomb PA, Gallinger S, Conti D, Schumacher F, Casey G, Taipale J, Cheadle JP, Dunlop MG, Tomlinson IP, Aaltonen LA, Houlston RS. Variation at 2q35 (PNKD and TMBIM1) influences colorectal cancer risk and identifies a pleiotropic effect with inflammatory bowel disease. Hum Mol Genet 2016; 25(11): 2349–2359
70. Gregersen LH, Mitter R, Ugalde AP, Nojima T, Proudfoot NJ, Agami R, Stewart A, Svejstrup JQ. SCAF4 and SCAF8, mRNA anti-terminator proteins. Cell 2019; 177(7): 1797–1813
71. Bishop GA. TRAF3 as a powerful and multitalented regulator of lymphocyte functions. J Leukoc Biol 2016; 100(5): 919–926
72. Sun X, Zhang H, Wang D, Ma D, Shen Y, Shang Y. DLP, a novel Dim1 family protein implicated in pre-mRNA splicing and cell cycle progression. J Biol Chem 2004; 279(31): 32839–32847
73. Yao X, Yan C, Zhang L, Li Y, Wan Q. LncRNA ENST00113 promotes proliferation, survival, and migration by activating PI3K/Akt/mTOR signaling pathway in atherosclerosis. Medicine (Baltimore) 2018; 97(16): e0473
74. Tian ZH, Yuan C, Yang K, Gao XL. Systematic identification of key genes and pathways in clear cell renal cell carcinoma on bioinformatics analysis. Ann Transl Med 2019; 7(5): 89